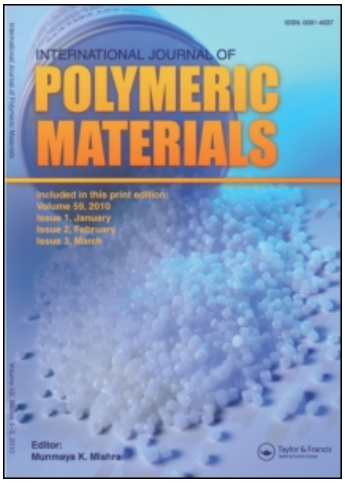

International Journal of Polymeric Materials
Publication details, including instructions for authors and subscription information:
http://www.informaworld.com/smpp/title~content=t713647664

Relationship between Melting Thermodynamics and Strength for Ultradrawn Polymers

V. A. Bershtein[a]; V. M. Egorov[a]; V. A. Marikhin[a]; L. P. Myasnikova[a]
[a] Ioffe Physico-Technical Institute, Russian Academy of Sciences, St. Petersburg, Russia

To cite this Article Bershtein, V. A. , Egorov, V. M. , Marikhin, V. A. and Myasnikova, L. P.(1993) 'Relationship between Melting Thermodynamics and Strength for Ultradrawn Polymers', International Journal of Polymeric Materials, 22: 1, 167 — 176
To link to this Article: DOI: 10.1080/00914039308012071
URL: http://dx.doi.org/10.1080/00914039308012071

Intern. J. Polymeric Mater., 1993, Vol. 22, pp. 167–176
Reprints available directly from the publisher
Photocopying permitted by license only

Printed in Malaysia

Relationship between Melting Thermodynamics and Strength for Ultradrawn Polymers

V. A. BERSHTEIN, V. M. EGOROV, V. A. MARIKHIN, and L. P. MYASNIKOVA

Ioffe Physico-Technical Institute, Russian Academy of Sciences, 26 Polytekhnicheskaya, St. Petersburg 194021, Russia

With the help of DSC, WAXS, and SAXS techniques highly oriented PE samples produced in six different ways in the range of draw ratios from 25 up to 300 have been investigated. The decrease of melting interval up to zero and the significant increase of melting temperature up to its equilibrium value are observed with draw ratio. The analysis of DSC data enabled us to calculate the thermodynamical parameter of intrachain cooperativity of melting which was found to be equal to $\nu \approx 2 \times 10^3$ nm. Although the observed thermodynamical characteristics corresponded to those expected for hypothetical macroscopic single crystals of PE, the combining of DSC and X-ray data allow to consider ultraoriented PE as consisting almost entirely of very extended (up to $\nu \approx 2 \times 10^3$ nm) straightened chain sections, each of which going through dozens of small crystallites and intercrystalline regions containing defects of disclinational type. As a result, the linear correlation between the parameter ν and the mechanical strength σ of oriented PE has been revealed.

KEY WORDS Oriented polyethylene, scanning calorimetry, melting behavior, structure/property relationships.

INTRODUCTION

Melt crystallized or solution-cast flexible-chain polymers exhibit tensile strengths and moduli of elasticity well below those calculated theoretically for an individual straightened long-chain molecule. Various techniques have been suggested to enhance their mechanical properties.[1] Their main aim was to straighten the flexible molecules and align them in one direction so as to use their mechanical potentiality to the best advantage. The oriented polymers have typically a microfibrillar structure consisting of microfibrils, thread-like units hundreds of angstroms in diameter, and ordered (crystalline) and disordered regions alternating along their longitudinal axes. The latter play an extremely important role in the mechanical behavior of polymers, being the weakest sites of material where all conformational defects, cilia and folds, are localized. Strength of the oriented polymer depends on the degree of orientation and the number of taut tie molecules.[1]

The structure of disordered regions can be studied by a great number of direct and indirect experimental techniques. Thus valuable information on disordered regions can be obtained from both the DSC data on increasing molecular mobility in these regions with temperature growth and from the DSC data on melting of crystalline regions.[2] The matter is that polymer crystallites do not form a separate extended phase but are interconnected by the segments of chain molecules incorporated both in the crystalline and disordered

TABLE I
Mechanical, structural and thermal characteristics of oriented PE prepared by different techniques

Preparation technique	$\bar{M}_w \times 10^{-6}$ (kg kmol^{-1})	λ	$\bar{D}_{002}$ (nm)	L (nm)	σ (GPa)	E (GPa)	T_m^t (K)	ΔT_m^t (K)
I	1.5	2.5	65	56	5.0	110	414	0.4–0.5
II	3.5	200	80	—	6.0	130	414	0.05–0.07
III	1.5	150	—	—	7.0	144	415	0.04–0.05
IV	4.5	300	55	—	6.0	—	417.5	0.05–0.07
V	0.1	25	32	25	0.5	70	408	1.8
VI	0.1	30	33	—	1.5	66	409	0.3–0.4

I. Multistage zone drawing of shish-kebab threads prepared from agitated solution by the Pennings technique.[4,5]
II. Multistage zone drawing of films prepared from gel by the Smith and Lemstra technique.[6]
III. Multistage zone drawing of the fibers prepared by technique II.[7,8]
IV. Solid-phase extrusion of the single crystal mats by the Porter technique[9] with a six-fold drawing by the Kanamoto technique.[10]
V. Solid-phase extrusion of a slowly crystallized melt by the Porter technique.[9]
VI. Multistage zone drawing of the quenched melt-crystallized films by Marikhin's and Myasnikova's technique.[11]

regions. This allows to assume that the thermal behavior of polymer crystallites must be affected by the amount of tie molecules and their conformations, as well as by the number of cilia and folds in intercrystalline disordered regions governing the mechanical properties. This implies that there exists some correlation between melting parameters and mechanical behavior of polymer, which was confirmed by the preliminary data.[3]

The aim of this work was to study the correlation between the melting thermodynamics and mechanical characteristics of highly oriented PE samples produced in different ways.

EXPERIMENTAL

The objects under study were samples of PE with $\bar{M}_w = (0.1\text{–}4.5)\times 10^6$ kg kmol^{-1} in the form of fibers, films, filaments or thin rods prepared by six well-known techniques listed in Table I. In the general case, the draw ratio λ varied from 2.5 to 300. For comparison, an initial isotropic PE ($\lambda = 1$) was also measured. Table I lists $\bar{M}_w$, ultimate λ attained for each technique, mechanical, structural and thermodynamical data of the samples under investigation.

Thermal measurements were performed by a DSC-2 Perkin–Elmer calorimeter calibrated with the melting temperatures of indium (429.7 K) and ice (273.1 K) as well as by the heat capacity of sapphire.

As is known, the magnitudes of T_m corresponding to the maximum of the endothermal melting peak and of the melting interval $\Delta T_m = T_2 - T_1$ on the DSC curve (Figure 1) obtained at certain heating rate v can be appreciably overestimated due to the thermal lag (at high v) or structural instability of polymer samples (at low v). In these cases[12] the error is proportional to $v^{1/2}$ and sample mass m. For this reason the true values of T_m^t and ΔT_m^t were obtained by scanning at different rates $v = 0.3\text{–}20$ deg min^{-1} and extrapolating the linear dependences of $T_m(v^{1/2})$, $T_1(v^{1/2})$, and $T_2(v^{1/2})$ to $v = 0$. It was difficult to find very small ΔT_m^t values by data extrapolation for ultimately oriented samples, and it was assumed in these cases that $\Delta T_m^t = \Delta T_m$ at $v = 0.3$ deg min^{-1}. In addition, to decrease the scatter in data, the PE samples of weight $m = 0.01\text{–}0.1$ mg were placed in a capsule

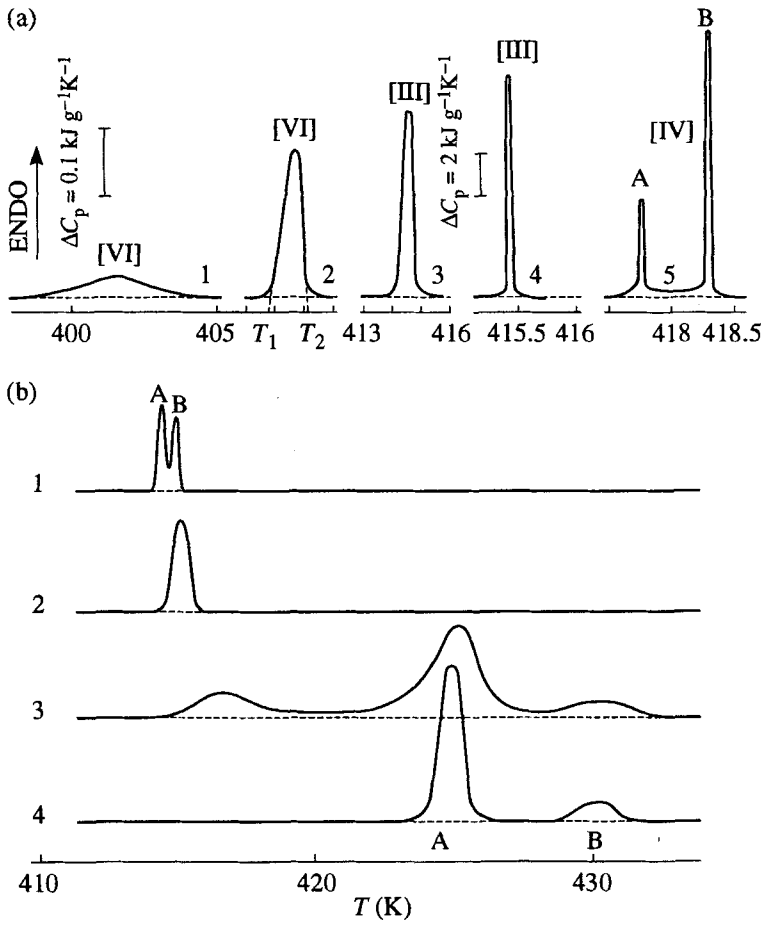

FIGURE 1 DSC curves for PE samples. (a) "Free" samples at heating rate $v = 0.3$ deg min^{-1} and various λ: 1 (curve 1), 30 (curve 2), 60 (curve 3), 150 (curve 4), and 300 (curve 5). The technique of sample preparation is shown in parentheses near curves. (b) PE fibers with $\lambda = 80$ obtained by technique III, heating rate $v = 1.25$ deg min^{-1}: free fiber, $m = 0.01$ mg (curve 1); ditto, $m = 0.4$ mg (curve 2); pressed in capsule (curve 3); constrained fiber with fixed ends (curve 4).

into a heat conducting medium of Wood's alloy with $T_m = 346$ K in a free state. As will be shown below, the thermal measurements of the samples in the constrained state produced randomly or in a special way gave rise to special melting effects.

The enthalpy of melting ΔH_m and degree of crystallinity $\chi_{DSC} = \Delta H_m / \Delta H_m^0$ where $\Delta H_m^0 = 4.1$ kJ mol^{-1} of CH_2 groups is the enthalpy of melting for an equilibrium perfect PE crystal[13] were also found from the endothermal melting peak area.

The information obtained was used to estimate two more parameters that appeared to be of special importance for understanding of an ultraoriented ultrahigh strength state of PE, viz. the parameter of an intrachain cooperativity of melting ν and free energy of the interfacial end surfaces of crystallites γ_i.

In addition to studying thermal properties, the longitudinal (along the c-axis) $\bar{D}_{002}$ and transverse $\bar{D}_{110}$ sizes of crystallites were calculated from broadening of the X-ray

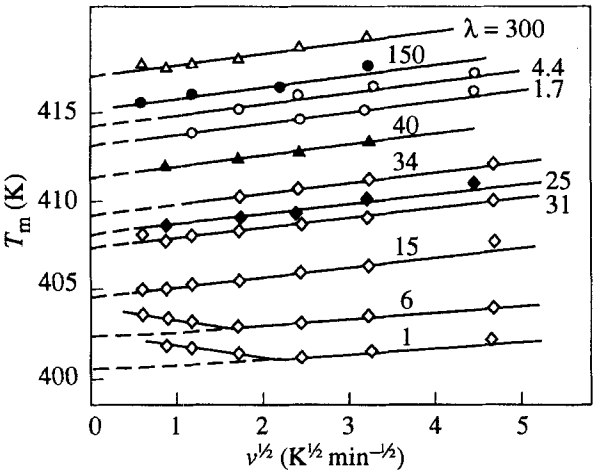

FIGURE 2 The T_m versus heating rate for PE samples oriented by different techniques listed in Table I: I (○), II (▲), III (●), IV (△), V (◆), and VI (◇). Draw ratio λ is shown near the curves.

diffraction peaks, and the long period L was found from small-angle photo X-ray patterns. All these data were compared with the strength σ and static modulus of elasticity E of the samples.

CALORIMETRIC DATA

Figure 1 shows the endothermal melting peaks for an initial PE sample and those oriented to different degrees using various techniques. The dependences of measured T_m versus the heating rate are shown in Figure 2. Table I gives the true values of T_m^t and ΔT_m^t for PE samples ultimately oriented by six techniques. Let us analyze the observed effects.

Melting of polymers is typically characterized by spreading of the phase transition when ΔT_m is sometimes 10 K or more, and by the reduced temperatures $T_m < T_m^0$ where T_m^0 is the equilibrium melting temperature of an "infinite" crystal; the T_m value depends on crystallization conditions. As shown in Figure 1, that is valid for an isotropic PE but as the draw ratio increases, T_m grows and the endothermal melting peak becomes higher and more narrow.

It has been found[14] that in case of ultraoriented PE the polymer crystallites melted, in fact, at one definite temperature ("at a point"). For instance, peak on curve 4 (Figure 1a), indeed, equals about 0.05 K in width, i.e. it is by two orders of magnitude narrower and higher than for the isotropic PE. In this case the equality of T_m^t to T_m^0 is reached, the latter is estimated to be 416 ± 2 K by different authors.[13,15,16]

As the orientation degree of PE grows, the experimental $T_m(v^{1/2})$ dependences are displaced toward higher temperatures almost without changes in their slope. The deviations of these curves from linearity are observed only at the initial stages of drawing at low v, i.e. when the fibrillar crystalline structure being formed is still unstable. The effect of thermal lag on passing from $v = 0$ to $v = 20$ deg min^{-1} is as low as 2–3 K owing to the heat conducting medium used and to the small weight of the samples (Figure 2).

Consequently, the ultraoriented PE can melt at an equilibrium temperature and within a "zero melting interval", i.e. similar to melting of crystalline solids of the other classes.

The achieved T_m^t and ΔT_m^t values correspond to those expected for hypothetical perfect macroscopic single crystals of PE. However, the degree of crystallinity χ_{DSC} of the samples studied did not exceed 87% in all the cases.

Another effect exhibited by ultraoriented PE samples was the manifestation of two stages of melting[14] which had been predicted theoretically by Flory.[13] They are (i) some disturbance of the intermolecular order (decrease in intermolecular interactions) and (ii) the intramolecular transition from a straightened (*trans*) conformation of molecules in a crystallite to the statistical coils in the melt.

As seen from Figure 1, at $v = 0.3$ deg min^{-1} (technique IV) and 1.25 deg min^{-1} (technique III), a splitting of the narrow melting peak into peaks A and B with a distance between them of about 0.5 K is observed for "free" samples owing to a high resolution of the DSC technique used. At elevated heating rates and (or) increased weights of the samples, no splitting occurs because of the instrumental broadening and overlapping of the peaks caused by the thermal lag (Figure 1b, curve 2).

A different picture was observed when the constrained ultraoriented samples were being heated.[14] When the samples of $m = 0.4$ mg were constrained by winding on an aluminium foil and fixing the ends, the DSC curves exhibited two rather broad new peaks A and B displaced toward higher temperatures (Figure 1b, curve 4). If the sample was merely tightly packed into a capsule (nonuniform fixing), an intermediate case could take place, and three melting peaks arose, one of them being close by its position to the initial one (Figure 1b, curve 3). The shifted peaks were manifest at $T_m^t = 424$ and 428 K at $v \to 0$.

As shown, the appearance of the doublet peak of melting (A and B) on the DSC curves for both short free and long constrained samples corresponds to two above stages and is not associated with the instability of crystallites.[14] It has been found that ultraoriented samples remained of the same length after passing only through melting peak A and subsequent cooling (a decrease in intermolecular interactions). They contracted transforming into a droplet only after passing through peak B (coiling of macromolecules).

Another explanation of two peaks observed also in melting of fixed fibers of highly oriented PE in References 17,18 was a transition from an orthorhombic structure of crystallites into a hexagonal one and then into a melt. This does not contradict to the first assumption, because the hexagonal structure is characterized, indeed, by a reduced intermolecular interaction, elevation in specific volume and molecular mobility.

The increase of T_m^t in case of the ultraoriented constrained sample up to temperatures above T_m^0 is caused by tensile stresses, emerging therein during heating, since such a sample has a negative thermal expansion coefficient.[19] The above data enabled estimation of T_m^t and ΔT_m^t values from peak B for ultraoriented samples that exhibit a melting doublet.

According to the Thomson–Gibbs equation

$$T_m^t = T_m^0 \left(1 - \frac{2\gamma_i}{\Delta H_m^0 \rho_{cr} \bar{D}_{002}} - \frac{4\gamma}{\Delta H_m^0 \rho_{cr} \bar{D}_{110}}\right), \quad (1)$$

where γ is the free energy of the lateral surfaces of crystallites ($\gamma \approx 10$ erg cm^{-2} for PE).[13] Since $\bar{D}_{002}$ and $\bar{D}_{110}$ change only slightly during drawing of PE (see below), the growth of T_m^t and especially $T_m^t \to T_m^0$ can mainly be explained by reduction of the free energy of end surfaces of crystallites γ_i that drops to zero in the limit. This points to an almost total disappearance of the interfacial boundary between the crystallite edge and intercrystalline region (absence of chain folding, etc.) in ultraoriented PE.

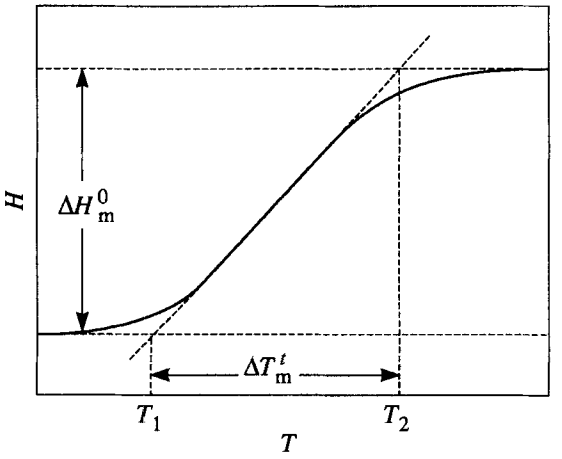

FIGURE 3 Scheme of change in the crystal enthalpy in the range of melting phase transition.

Melting of a polymer crystallite starts from the defect site at a lateral face and proceeds through the successive separation of chain portions in the direction perpendicular to the c-axis of the crystallite.[13] The shortest chain portion consisting of ν monomer units that passes as a whole from a crystallite into a statistical coil in the melt can be arbitrarily referred to as a "kinetic unit" of melting; then, this transformation can be considered as an "elementary act" of the process.

The value of ν is the parameter of intrachain cooperativity of the order-disorder type transition.[20,21] It can be estimated proceeding from the thermodynamic characteristics of melting, viz.

$$\nu = \frac{2R(T^t_m)^2}{\Delta T^t_m \Delta H}. \tag{2}$$

Here, R is the gas constant, and the value of ν is primarily determined by the melting interval width and a jump of enthalpy at transition, i.e. basically by a change in the energy of intermolecular interaction calculated per one mole of monomer units. In the first approximation $\Delta H = \Delta H^0_m$ (see the scheme in Figure 3). The higher the intramolecular cooperativity in the transition unit event, the more narrow the temperature interval within which it occurs.† It was found that the parameter ν for different isotropic PE samples approximately equals $\bar{D}_{002}$, i.e. it is close by magnitude to the thickness of lamellar crystallites.[22] At the same time, the estimates fulfilled for oriented and ultraoriented PE samples show that ν grows with drawing, the growth is much greater than that of crystallite thickness ν reaching 2×10^3 nm. Below we consider this result in relation to the structural data and strength.

† In some cases the second reason for elevated ΔT^t_m values, namely, a considerable dispersion of crystallite thicknesses ($\bar{D}_{002}$) should also be taken into account (Equation (1)).

RELATION OF MELTING PARAMETERS TO THE STRUCTURE AND STRENGTH

The measured thermal characteristics of melting of ultraoriented PE correspond to those expected for an equilibrium single crystal ($T_m^t = T_m^0$, $\Delta T_m^t \approx 0$). However, the X-ray studies have shown that the molecules in these samples do not form very extended regions of three-dimensional order (coherent scattering): the longitudinal size, i.e. the thickness of crystallites $\bar{D}_{002}$ grew from 10–20 nm in isotropic samples to merely 60–80 nm in ultraoriented PE (see Table I). Along with this, the observed values of $\Delta T_m^t \ll 1$ K point not only to the absence of a considerable dispersion of crystallite thicknesses but also to the fact that the macromolecules in ultraoriented samples consist mainly of the straightened (*trans*) sections in length up to 2×10^3 nm, which greatly exceeds the longitudinal size of crystallite $\bar{D}_{002}$.

The value of $\bar{D}_{002}$ in the structure of the samples studied (for more details see Reference 23) was much larger than the long period L already at $\lambda \leq 25$, and for samples in the ultraoriented state the long period was absent (see Table I). The density of the disordered regions approached the density of crystallites that was indicated by disappearance of small-angle X-ray reflections. From the one-dimensional X-ray diffraction data[24] one might expect that the highly oriented PE contained the straightened molecular fragments of the effective longitudinal size larger than L.

Figure 4 shows schematically the molecular structure of intercrystalline regions in isotropic, oriented, and ultraoriented PE. In the isotropic samples these regions have a peculiar and complex conformational structure. A difference in lengths of chain sections connecting the crystallites, formation of regular folds and loose loops, and other features are responsible for a wide distribution of temperatures of segmental mobility unfreezing and manifestation of four relaxation regions.[26]

In oriented samples the content of loops in disordered regions is negligibly low, the number of load-bearing straightened tie chains increases, and a considerable amount of chains with conformational and rotational defects is preserved.

As shown by the data obtained, the ultraoriented PE consists almost entirely of very extended *trans*-sequences of the repeated units, each of which goes through dozens of crystallites and intercrystalline regions and passes at T_m in one step from the extended state into a coil ($\nu \approx 2 \times 10^3$ nm).

Disturbance of the three-dimensional order in the intercrystalline regions is likely to be limited in this case only by the molecular packing defects of the type of disclinations with rotation of chain segments, etc. These defects cause a certain azimuthal disorder, viz. the planes of straightened chain sections become nonparallel. That is why the X-ray technique identifies the intercrystalline regions in ultraoriented PE as disordered ones, and DSC regards these samples as the defect single crystals. The latter can be inferred from the observed values of T_m^t, ΔT_m^t, and ν, and by taking into account that $\gamma_i \rightarrow 0$ and $\chi \leq 90$ %. Note that the X-ray degree of crystallinity χ_{WAXS} is less than χ_{DSC}.[25,26]

Hence, the thermodynamic parameter ν is a characteristic of orientation, the straightened state of tie chains in PE and therefore it must be connected with the mechanical strength σ.

Figure 5 shows the experimental dependences of T_m^t, χ_{DSC}, and σ on draw ratio of PE samples obtained by techniques II–VI (see Table I).

It is obvious that the first two parameters increase with growing λ somewhat differently

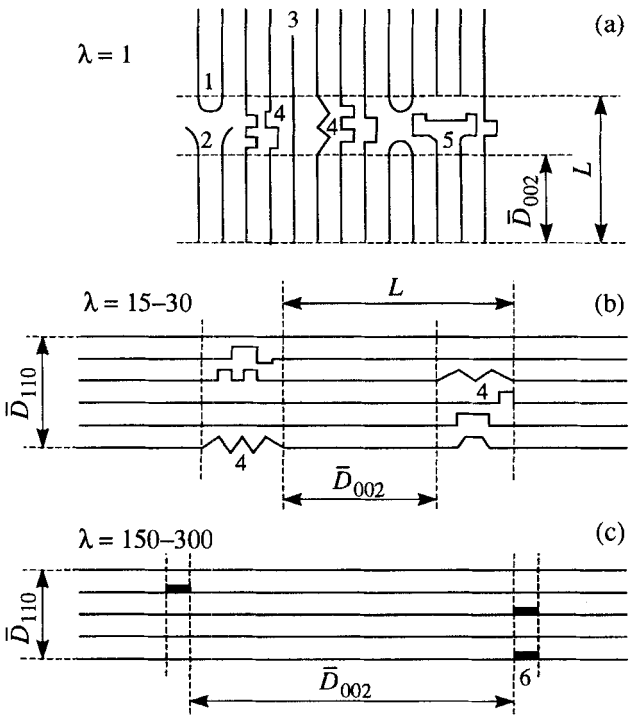

FIGURE 4 Schematic presentation of the molecular structure of intercrystalline regions for (a) isotropic, (b) oriented, and (c) ultraoriented PE. 1, regular fold; 2, cilia; 3, extended chain segments; 4, bent tie chain with conformational or rotational defects; 5, loose loops; 6, disclination defects.

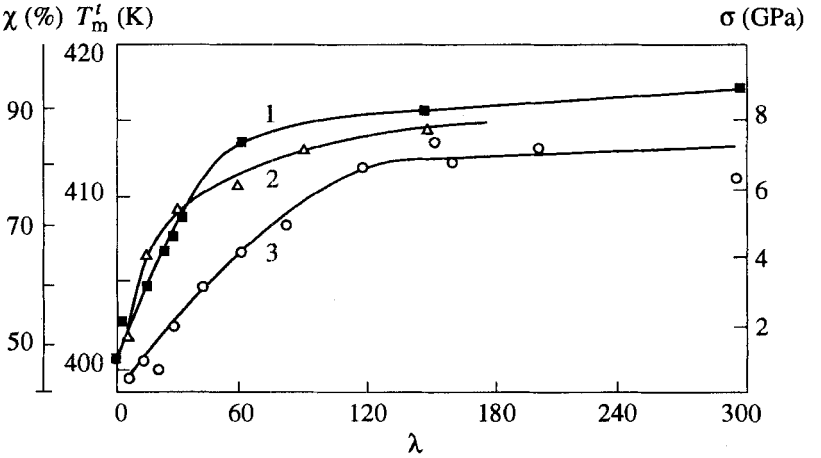

FIGURE 5 Melting temperature (curve 1), degree of crystallinity from DSC data (curve 2), and strength at 293 K (curve 3) as functions of draw ratio for PE samples.

than the strength. For instance, T_m^t reaches $T_m^0 = 416 \pm 2$ K as early as at $\lambda = 60$, $\chi = 85$–87% at $\lambda = 90$, but the strength σ reaches at 293 K its maximum value of 6–7 GPa only

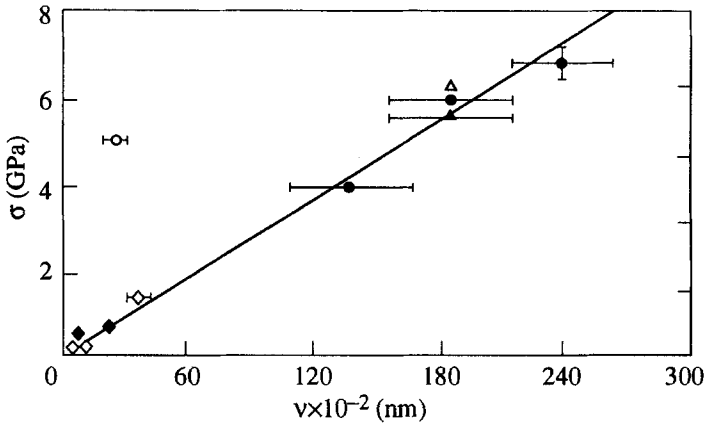

FIGURE 6 Strength of oriented and ultraoriented PE prepared by techniques I–VI as a function of parameter of intrachain cooperativity of melting ν. I (○), II (▲), III (●), IV (△), V (◆), and VI (◇).

at $\lambda = 120$ remaining then unaltered up to $\lambda = 300$. According to Reference 7, at 77 K the magnitudes of $\sigma = 10$ GPa and $E = 210$ GPa, close to the theoretical estimates of $\sigma_{th} = 12$–15 GPa and $E_{th} = 240$–250 GPa,[7,8,19] have been obtained for samples obtained by technique III. As is seen from Table I, samples obtained by technique V and VI with a relatively low $\bar{M}_w$ and the moderate draw ratios λ exhibit the lowest σ and E values.

A linear correlation between the strength and parameter of intrachain cooperativity of melting ν was found (Figure 6) for PE samples of all the types with the exception of the samples obtained by technique I that had a peculiar composite ("shish-kebab") structure. They undergo orientation already in the process of preparation of initial samples from the stirred solution and are additionally stretched only 2–4 times by zone drawing.

However, the presence of crystallites with straightened chains in their structure led to fairly high strengths and moduli of elasticity (see Table I).

This suggests that the parameter ν as a characteristic of the *trans*-state of tie chains in oriented PE is directly related to strength. The significance of this result lies in the fact that a direct correlation between thermodynamics of melting and mechanical strength of oriented and ultraoriented polymers has been revealed for the first time.

CONCLUSION

The comparative analysis of X-ray and DSC data obtained for highly oriented PE samples produced in six different ways enabled us to establish a difference in their fine structure.

It was found that they differ in a length of extended fragments of macromolecules, which is extremely important for the mechanical properties. Linear correlation between the length of these fragments, determined as parameter of an intrachain cooperativity of melting ν was established. The difference in crystallite sizes was found to play a minor (or secondary) role. The longest *trans*-sequences are present in the strongest gel-crystallized drawn UHMWPE sample and reach 2×10^3 nm in length, which is comparable with that of a whole macromolecules.

X-ray study used in combination with the DSC technique is considered to be very useful for understanding the fine structural organization of polymers.

References

1. V. A. Marikhin and L. P. Myasnikova, *Supermolecular Structure of Polymers*, (Khimiya, Leningrad, 1977) (in Russian).
2. V. A. Bershtein and V. M. Egorov, *Differential Scanning Calorimetry of Polymers*, (Ellis Horwood, Chichester, 1993).
3. B. A. Bershtein, V. M. Egorov, V. A. Marikhin, and L. P. Myasnikova, *Preprints of IVth Intern. Symp. on Chem. Fibers*, (Kalinin, 1986), Vol. 1, p. 132.
4. J. Smook, J. Toorts, P. Van Hutten, and A. Pennings, *Polym. Bull.*, **2,** 293 (1980).
5. V. A. Marikhin, L. P. Myasnikova, D. Zenke, R. Hirte, and P. Weigel, *Vysokomol. Soedinen.*, **B26,** 210 (1984).
6. P. Smith and P. Lemstra, *Makromol. Chem., Rapid Commun.*, **180,** 2983 (1979).
7. A. V. Savitsky, I. A. Gorshkova, G. N. Shmick, and I. L. Phrolova, *Vysokomol. Soedinen.*, **B25,** 352 (1983).
8. A. V. Savitsky, I. A. Gorshkova, V. P. Demicheva, J. L. Phrolova, and G. N. Shmick, *Vysokomol. Soedinen.*, **B26,** 1801 (1984).
9. R. Porter, J. Southern, and N. Weeks, *Polym. Eng. Sci.*, **15,** 313 (1975).
10. T. Kanamoto, A. Tsaruta, K. Tanaka, M. Takeda, and R. Porter, *Polymer*, **15,** 327 (1983).
11. L. A. Gann, V. A. Marikhin, L. P. Myasnikova, V. P. Budtov, G. D. Myasnikov, and E. L. Ponomareva, *Vysokomol. Soedinen.*, **A29,** 1658 (1987).
12. K. Illers, *European Polym. J.*, **10,** 911 (1974).
13. B. Wunderlich, *Macromolecular Physics. Crystal Melting*, (Academic Press, New York, 1980).
14. V. A. Bershtein, A. V. Savitsky, V. M. Egorov, I. A. Gorshkova, and V. P. Demicheva, *Polym. Bull.*, **12,** 165 (1984).
15. Yu. K. Godovsky, *Encyclopedia of Polymers*, (Sov. Entsiklopediya, Moskow, 1974) Vol. 2, p. 607 (in Russian).
16. V. P. Privalko, *Molecular Structure and Properties of Polymers*, (Khimiya, Leningrad, 1986) (in Russian).
17. A. Pennings and A. Zwijnenburg, *J. Polym. Sci., Polym. Phys. Ed.*, **17,** 1011 (1979).
18. J. Smook and A. Pennings, *Colloid and Polym. Sci.*, **262,** 712 (1984).
19. Yu. K. Godovsky, *Thermophysics of Polymers*, (Khimiya, Moscow, 1982) (in Russian).
20. P. Flory, *Proc. Royal Soc.*, **49,** 105 (1961).
21. S. Yu. Frenkel, *Encyclopedia of Polymers*, (Sov. Entsiklopediya, Moscow, 1974) Vol. 2, p. 128 (in Russian).
22. V. A. Marikhin, V. A. Bershtein, V. M. Egorov, and L. P. Myasnikova, *Vysokomol. Soedinen.*, **A28,** 1983 (1986).
23. V. A. Marikhin and L. P. Myasnikova, *Makromol. Chem., Macromol. Symp.*, **41,** 209 (1991).
24. S. N. Chvalun, V. S. Shiretz, Yu. A. Zubov, and N. F. Bakeev, *Vysokomol. Soedinen.*, **A28,** 18 (1986).
25. S. N. Chvalun, M. B. Konstantinopolskaya, E. A. Sinevitch, N. P. Bessonova, Yu. A. Zubov, and N. F. Bakeev, *Preprints of IVth Intern. Symp. on Chem. Fibers*, (Kalinin, 1986), Vol. 1, p. 97.
26. V. A. Bershtein, V. M. Egorov, V. A. Marikhin, and L. P. Myasnikova, *Vysokomol. Soedinen.*, **A27,** 771 (1985).